Localization phenomena in elastic surface-polariton scattering caused by surface roughness

Sergey I. Bozhevolnyi
Institute of Physics, Aalborg University, Pontoppidanstræde 103, DK-9220 Aalborg, Denmark
(Received 12 February 1996)

Localization phenomena in the elastic scattering of surface plasmon polaritons (SPP's), i.e., in the SPP scattering in the surface plane, are related to the appropriate characteristics of SPP and surface roughness. Optical fields of SPP's, which are excited at two different wavelengths (488 and 633 nm) used in turn for each surface region of four different metal (silver and gold) films, are imaged simultaneously with surface topography by use of a photon scanning tunneling microscope with shear force feedback. Single scattering and weak and strong localization of SPP's are observed depending on the sample and the light wavelength. This is a direct demonstration of different regimes of the elastic SPP scattering realized at the same surface region for different light wavelengths. It is shown that the regime of SPP scattering and, consequently, near-field optical images, are determined by the topography of a local surface area with the size limited by the SPP propagation length. [S0163-1829(96)00935-6]

I. INTRODUCTION

Localization of light is an essentially interference phenomenon related to multiple elastic scattering in random media.[1,2] When a wave propagates through a strong-scattering and nonabsorbing random medium, the mean free path is reduced due to interference in multiple scattering. Strong (Anderson) localization implies that the mean free path vanishes and propagation no longer exists—the wave is captured in a ''random'' cavity. For electrons this is a well-studied phenomenon, but it has not yet been observed unequivocally for light waves in three dimensions. The problem is that the scattering potential is frequency dependent for electromagnetic waves, a circumstance which leads to the divergence of the mean free path in the limit of both low and high frequencies.[3] This means, in turn, that the Ioffe-Regel condition for localization, viz. $2\pi/\lambda \sim 1$, with λ being the wavelength of light and l being the elastic scattering mean free path, is extremely difficult to realize. Another interference phenomenon that has been observed and extensively studied is enhanced backscattering (also referred to as weak localization), which is already present in lower orders of multiple scattering, and considered to be a precursor of strong localization.[4,5] The weak-localization effect arises from a constructive interference (in the backscattering direction) between two waves scattered along the same path in opposite directions, and, therefore, shows up already in double scattering.

The situation with localization is completely different in two dimensions: light,[3] as well as electrons,[6] is localized with any degree of disorder, at least in the absence of absorption. Qualitatively, it can be explained by the fact that a random walk is recurrent in two dimensions, implying that the effective cross section of a single scatterer tends to infinity, drastically reducing the effective mean free path.[1] Surface plasmon polaritons (SPP's) propagating along a plane interface represent (quasi) two-dimensional waves, and, therefore, should exhibit localization effects caused by surface roughness.[7] Traditionally, interaction of SPP's with surface roughness has been investigated by using far-field measurements of light scattered into a free space.[8] It should be stressed that, here, our consideration is concerned with the (elastic) SPP scattering in the surface plane, and that SPP scattering into a free space is an unwanted process leading to the additional (radiative) losses experienced by the SPP. In passing we note that the coupling between SPP's and propagating (in air) field components due to surface roughness is responsible for the remarkable phenomenon of backscattering enhancement in the diffusely scattered (out of the surface plane) light.[9] Localization phenomena related to elastic SPP scattering are difficult to observe because of the spatial confinement of the SPP field in the direction perpendicular to the surface plane. Indirectly, weak localization of SPP's has been observed by detecting a sharp peak in the angular dependence of the efficiency of second-harmonic generation (SHG) in the direction perpendicular to the sample surface.[10] Such a peak is a manifestation of the enhanced backscattering of SPP's, since SHG in the normal direction is related to the nonlinear interaction between counterpropagating (i.e., between the excited and backscattered) SPP's at the fundamental frequency.[11] Only with the advent of scanning probe techniques did it become possible to probe (with high spatial resolution) the SPP field directly and locally, thus opening additional possibilities for studying the SPP scattering in the surface plane.

Recently developed photon scanning tunneling microscope (PSTM),[12] in which an uncoated fiber tip is used to detect an evanescent field of the light being totally internally reflected at the sample surface, is apparently the most suitable technique for local probing of the SPP field, especially when combined with shear force feedback for regulation of the tip-surface distance. Due to the relatively low refractive index of optical fiber, such a tip can be within certain approximations considered as a nonperturbative probe of the electric-field intensity,[13,14] and such a feedback system provides a possibility to measure the surface topography simultaneously with the near-field intensity distribution in the surface plane.[15,16] The PSTM has already been used in various studies concerned with the SPP characteristics[17] as well as

with the elastic SPP scattering caused by surface roughness.[18–20] In the latter studies, the scattering of SPP's (at a wavelength of 633 nm) propagating along different film surfaces with different roughnesses has been investigated by using the PSTM with shear force feedback. It has been observed that near-field optical images, which are generated due to the SPP propagating along a rough gold surface, exhibit spatially localized (within 150–250 nm) intensity enhancement by up to seven times,[18,19] whereas those due to the SPP at a relatively smooth gold surface show a well-pronounced interference pattern related to the interference between the excited and scattered SPP's.[18] The SPP scattering at silver surfaces has been found to produce the back-scattered SPP, which showed up in near-field optical images in the form of interference fringes oriented perpendicular to the excited SPP.[20] The observed difference in the scattering regimes for different films indicates that the SPP localization does not occur automatically at a rough surface.

Here, SPP characteristics and surface roughness are considered in connection with localization effects in the elastic SPP scattering. An experimental study of different scattering regimes is carried out by using the PSTM with shear force feedback. Near-field optical images generated due to SPP's excited at different surfaces of gold and silver films are obtained with two different wavelengths (488 and 633 nm) used in turn for each surface region studied. Single scattering, and weak and strong localization of SPP's are observed depending on the sample and the light wavelength. It is directly demonstrated that different regimes of the elastic SPP scattering can be realized at the same surface region by changing the light wavelength.

II. DISCUSSION

According to the scaling theory of localization,[3,6] two-dimensional waves are localized in the absence of absorption with any degree of disorder. The situation with SPP's is different for several reasons. First and foremost, SPP's, being confined in the direction perpendicular to the surface plane, are quasi-two-dimensional waves. This means that, in general, any surface inhomogeneity leads not only to the elastic SPP scattering, which is a cause of localization, but also to the (inelastic) SPP scattering out of the surface plane. The latter process gives rise to radiative losses, thereby decreasing the length of the SPP propagation path. However, even for a perfectly flat interface between air and a homogeneous metal, the SPP propagation length L is finite due to the internal damping. In the case of semi-infinite media on both sides of the air-metal interface, the SPP propagation length (or the lateral decay length) is given by

$$L=\lambda\left[4\pi\mathrm{Im}\left(\frac{\varepsilon}{\varepsilon+1}\right)^{1/2}\right]^{-1}, \tag{1}$$

where ε is the dielectric constant of metal. Usually, SPP's are excited at the air-metal interface of a thin metal layer placed on the surface of a glass (or silica) prism by using the light beam incident from the side of the prism, i.e., in the Kretschmann configuration.[21] In such a case, the SPP propagation length L is smaller than the one expressed by Eq. (1) due to the coupling between the SPP and the field components propagating in the prism, which results in the resonant reradiation of the SPP. For a realistic interface, L is further reduced due to the aforementioned inelastic scattering. However, for a standard vacuum-deposited metal layer, L is mainly determined by the first two processes, and one can use Eq. (1) for the estimation of L, keeping in mind the reduction of L due to the finite layer thickness.[22]

It is clear that the regime of multiple scattering of light associated with localization can be realized only if light paths are sufficiently long with respect to the elastic mean free path. In the case of weak localization of light, deterioration of the coherent backscattering peak by cutting off long light paths with absorption or confined geometry has been experimentally demonstrated.[23] The condition of weak dissipation of SPP's means accordingly that the SPP propagation length should be much larger than the elastic scattering mean free path: $L \gg l$.[7] However, this may not be enough to ensure strong localization of SPP's, especially with weak disorder ($l \gg \lambda_{sp}$, with λ_{sp} being the SPP wavelength).

In the weak-scattering limit, strong localization of light in two dimensions can be viewed as a consequence of the fact that, for a classical random walker, the total sojourn time in a small finite region around the origin is infinite.[1,2] In the presence of losses, the sojourn time T is apparently finite, and can be evaluated in the wavelength-sized region as follows:

$$T=\frac{\lambda^2}{4D\pi}\int_{l/c}^{L/c}\frac{dt}{t}=\frac{\lambda^2}{4D\pi}\ln\frac{L}{l}, \tag{2}$$

where D is the classical diffusion coefficient ($D\approx lc/3$), c is the speed of light in a medium, and L is the inelastic mean free path (the SPP propagation length in the case of SPP's). It seems reasonable to suggest that this time should be sufficiently large in comparison with the time l/c of free propagation in order for strong localization to occur. This condition leads to the following relation for the inelastic mean free path:

$$L \gg l\ \exp\left(\frac{4\pi l^2}{3\lambda^2}\right). \tag{3}$$

It is well known that the localization effects deteriorate when the size of the system becomes of the order of the localization length.[1] The influence of absorption on localization is similar to that of confined geometry,[23] and one should require L to be much larger than the localization length,[7] which can be evaluated as $\xi \sim l\ \exp(2\pi l/\lambda)$.[1,2] The fact that the condition $L \gg \xi$ is automatically fulfilled (for $l > \lambda$) once the relation expressed by Eq. (3) is satisfied, confirms the validity (at weak disorder) of the derived condition for strong localization. The exponential divergence of this condition with respect to the ratio l/λ means that the strong localization of light (in two dimensions) by weak disorder is a very problematic issue in the presence of losses.

In the case of SPP's, the SPP propagation length L in visible and near-infrared regions can be at best hundreds of μm, implying that the aforementioned condition [cf. Eq. (3)] cannot be satisfied at weak disorder ($l \gg \lambda_{sp}$). Therefore, strong localization of SPP's can be realized only at strong disorder ($l \sim \lambda_{sp}$). One can expect to find sufficiently strong disorder in the case of a film with an island structure similar

to that used for the first observation of strong SPP localization.[18,19] Consequently, at weak disorder, SPP's can exhibit only weak localization, i.e., of course if L is large enough to ensure at least double scattering: $L>l$. Such a condition is relatively easy to satisfy with noble metals, e.g., silver films have been used to observe weak localization effects in the SPP scattering.[10,20] Evaluation of the elastic mean free path l for SPP's is a challenging problem that is of interest in its own right. However, it can be roughly estimated by using the circumstance that standard metal films have smooth surfaces with rarely spaced μm-sized bumps.[18,20] Introducing the average bump size a and the average separation R between surface bumps, one can estimate l in the limit of geometrical optics ($a \gg \lambda_{sp}$) as $l \sim R^2/a$. Such an evaluation is convenient to use in near-field experiments, in which the surface topography is measured simultaneously with the SPP intensity distribution.[18–20] As the internal damping increases, the regime of multiple scattering (at weak disorder) changes to the regime of single scattering, when the following relation is valid: $l>L \gg \lambda_{sp}$. Finally, if $L \sim \lambda_{sp}$, then the SPP propagation and scattering in the surface plane become meaningless, even though the SPP excitation (in the Kretschmann configuration) can still be quite pronounced in the angular dependence of the reflected light power.

There are several specific features of near-field experiments with SPP's, which should be taken into account when looking for the localization effects in the elastic SPP scattering. First, it is very important that the SPP scattering into propagating (in air) field components should be sufficiently weak. This scattering decreases L, and contributes to the detected optical signal, thus distorting recorded images of the SPP intensity distribution. The second effect can be significantly decreased by using a proper fiber tip for the near-field detection, as will be discussed below. Second, the surface area that can be imaged is usually much smaller than the size of an incident laser beam used for the SPP excitation. This means that the image area should be inside the spot of the incident beam. Therefore, it seems hardly possible to measure transmission or reflection of the SPP through a corrugated region, as could have been suggested by extrapolating the ideas of experiments carried out in three dimensions. On the other hand, with near-field microscopy, there appears a unique opportunity to observe interference phenomena in the elastic SPP scattering directly by imagining the appropriate interference pattern. In the case of strong localization of SPP's, the near-field optical images are expected to exhibit bright spots.[18,19] The weak localization of SPP's is related to the formation of the backscattered SPP, which upon interference with the excited SPP should produce interference fringes perpendicular to the propagation direction of the excited SPP.[20] Finally, one should realize that the SP intensity in a particular surface region is determined by excitation and scattering of SPP's in the surrounding area within the SPP propagation length. Therefore, the aforementioned averaged characteristics of surface roughness (l,R,a) are of limited use, and the near-field optical images obtained with the same sample can be very much different for different surface regions.

III. EXPERIMENTAL TECHNIQUE

The experimental setup, which consists of the PSTM combined with the shear-force-based feedback system and an arrangement for SPP excitation in the usual Kretschmann configuration, is described in detail elsewhere.[18] The p-polarized (electrical field is parallel to the plane of incidence) light beam either from a He-Ne laser ($\lambda_1 \approx 633$ nm, $P_1 \approx 3$ mW) or from an argon-ion laser ($\lambda_2 \approx 488$ nm, $P_2 \approx 5$ mW) is used for the SPP excitation. Both incident beams can be alternatively directed and focused onto the base of a prism with a metal film (focal length ≈ 500 mm, spot size ~ 400 μm). The reflected light is detected by a photodiode, and the excitation of the SPP is recognized as a minimum in the angular dependence of the reflected light power (attenuated total reflection minimum.)[8,21] Both incident beams are angular adjusted in a way that ensures resonant SPP excitation for either of the two wavelengths. Commercially available optical glass prisms have been used as substrates for the studied films in order to facilitate the SPP excitation in the Kretschmann configuration.

The films are the same as those used in the previous studies.[18,20] The first gold film (film $G1$) with a thickness of 60 nm has been thermally evaporated under standard conditions (vacuum $\approx 10^{-6}$ Torr, evaporation speed ~ 1 Å/s). Typically, these conditions result is smooth metal films. In order to obtain a film with significantly larger surface roughness, the second gold film (film G2) with the thickness of 80 nm has been evaporated at a much greater speed (evaporation time $t \sim 1$ s) in a relatively poor vacuum ($\approx 10^{-5}$ Torr). The silver films (films $S1$ and $S2$) are of the same thickness of 45 nm, but with only slightly different roughnesses due to different fabrication conditions: film $S1$ has been evaporated under normal conditions (as film G1), whereas film $S2$ has been evaporated at the speed of ~ 5 Å/s in a vacuum of $\approx 5 \times 10^{-5}$-Torr pressure.

The SPP local field is probed with an uncoated fiber tip, which is fabricated by etching of a single-mode silica fiber in a 40% solution of hydrofluoric acid during a time period of 55 min.[24] Similar fiber tips have been used in previous studies of SPP propagation and scattering on gold films.[18–20] These tips are known to have a rather large cone angle (typically $\delta \approx 40°$).[24] The fiber cone angle is a very important characteristic of the fiber tip for studies of elastic SPP scattering, in which the SPP field should be effectively detected and discriminated from the propagating in air field components related to the inelastic SPP scattering. The SPP field is predominantly polarized in the direction perpendicular to the surface plane, whereas the propagating (in air) field contains components parallel to the surface plane. Considering the detection process as a detection of radiation from a pointlike dipole induced at the tip end into the fiber cone,[13] one can find that the detected signal related to the perpendicular field component increases more rapidly with the cone angle ($\sim \delta^4$, for small δ) than the one related to the parallel field components does ($\sim \delta^2$). Therefore, within the model approximations,[13] a larger cone angle should ensure a higher detection efficiency of the SPP field as well as a better discrimination against the propagating field components.

In the preliminary experiments, the SPP-related signal measured with a sharper fiber tip ($\delta \approx 10°$) was found to be

about two orders of magnitude weaker than the signal detected with the tip that we usually used ($\delta \approx 40^0$). The signal dependence on the tip-surface distance was also very different for these tips. The detected signal was typically more than 20 times smaller if the fiber tip was moved ~ 1 μm away from the surface of a smooth metal (gold or silver) film with the SPP being resonantly excited. Under similar circumstances, but with the aforementioned sharp tip, only a 60% decrease in the detected signal was measured. Neglecting the SPP field at a tip-surface distance of 1 μm, and assuming that the propagating field contains an appreciable amount of components parallel to the surface plane, one can see that the experimental results are in a good agreement with the above considerations. This also means that, contrary to detection with the sharp tip, the contribution of the propagating field components in the signal detected near the surface with our usual fiber tip is negligibly small in comparison with the SPP-related contribution. The previously observed interference patterns[18,20] showed a rather high contrast, and the period related to the SPP wavelength (which is less than the light wavelength in air). These observations are yet additional evidence supporting the above conclusion.

IV. EXPERIMENTAL RESULTS

For the studied films, angular dependences of the reflected light power at $\lambda_1 \approx 633$ nm have been previously measured and reported.[18,20] Similar dependences were also observed with the other light wavelength $\lambda_2 \approx 488$ nm. The SPP field intensity distributions near the surfaces of these samples were investigated by using the resonant excitation of SPP's at the two wavelengths in turn for each surface region studied. While imagining the SPP fields with the PSTM, the surface profiles were simultaneously determined by use of the shear force technique with a depth resolution of a few nanometers and a lateral resolution of better than 50 nm.[16] It should be noted that all images presented here are oriented in a way that the excited SPP propagates upwards in the vertical direction.

A. Gold films

Typographical images of film $G1$ showed a smooth surface with rarely spaced sized bumps [Fig. 1(a)]. The near-field optical images, which were generated due to the resonantly excited SPP at λ_1, usually exhibited a well-pronounced interference pattern related to the interference between the excited and scattered SPP's [Fig. 1(b)] (this phenomenon has been previously observed and discussed[18]). The appropriate near-field optical images due to the SPP at λ_2 were very different, and in most cases showed an intensity distribution correlated largely with the local surface topography [Fig. 1(c)]. Such a difference between the optical images recorded at the same place is explained by the fact that the SPP propagation length L is very different for these wavelengths. Using Eq. (1) and the available optical constants[25] accordingly results in $L_1 \approx 8$ μm and $L_2 \sim 0.4$ μm for λ_1 and λ_2. The average distance between surface scatterers was evaluated as $R \sim 7$ μm. Judging from the topographical images [Figs. 1(a) and 2(a) from this paper, Figs. 7(a) and 11(a) from Ref. 18], the average bump size

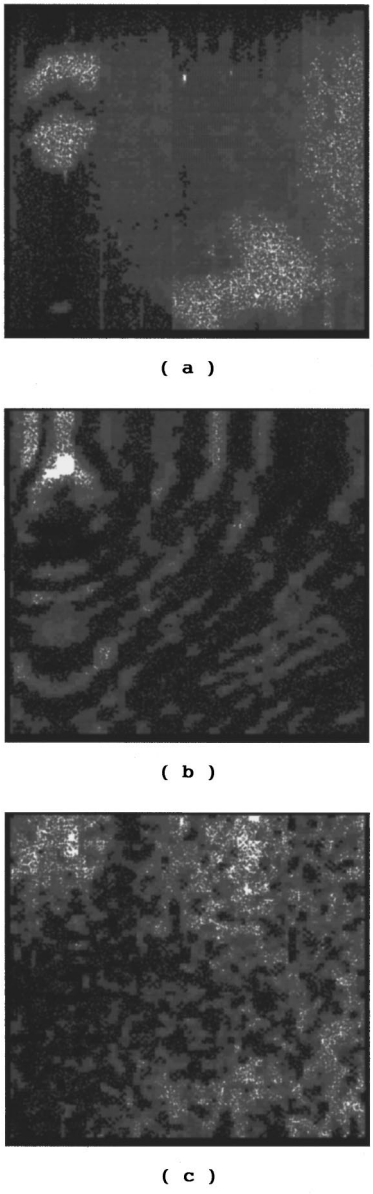

FIG. 1. Gray-scale topographical (a) and near-field optical (b) and (c) images 4×4 μm^2 obtained with film $G1$. The maximum depth of the topographical image is 66 nm. The optical images were taken at the same place with the polariton being resonantly excited at $\lambda_1 \approx 633$ nm (b) and $\lambda_2 \approx 488$ nm (c). The optical images are presented in different scales corresponding to ~ 0.015–1 (b) and 0.002–0.1 nW (c) of the detected optical signal.

can be estimated as $a \sim 1$ μm. Therefore, one can evaluate the elastic scattering mean free path as $l \sim 50$ μm (see Sec. II). Since $l \gg L_1 \gg \lambda_1$ and $l \gg L_2 \sim \lambda_2$, the regime of single scattering is usually realized with the first wavelength [Fig. 1(b)], whereas no scattering is expected for the second wavelength [Fig. 1(c)]. Another consequence of larger internal damping at λ_2 was a considerably smaller value (by ~ 10 times) of the average optical signal.

Scattering of the SPP by an individual surface feature is extremely difficult to analyze for realistic surfaces. One of the reasons is that the scattering process is strongly dependent on the scatterer's shape, which is more or less arbitrary and often rather complicated. In the course of this study, it was noticed that some bumps with smooth profiles did not

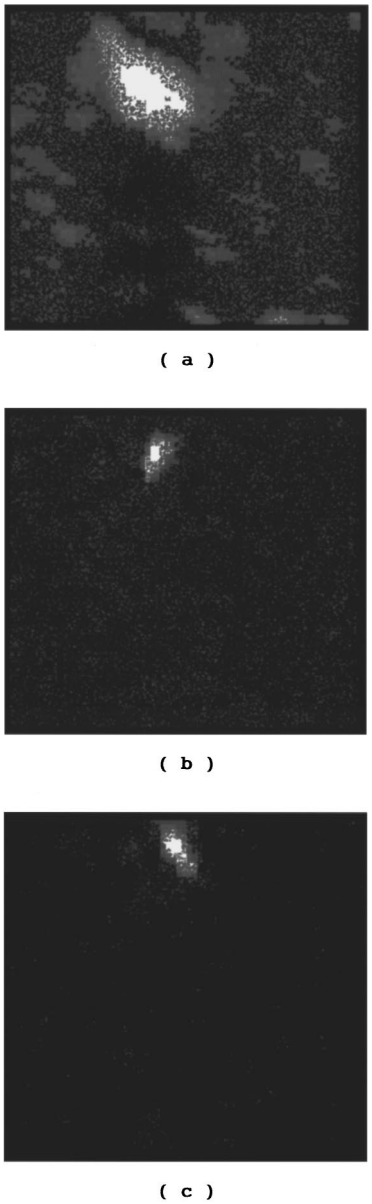

FIG. 2. Gray-scale topographical (a) and near-field optical (b) and (c) images 3×3 μm^2 obtained with film $G1$. The depth of the topographical image is 121 nm. The scales of optical images are $\sim$0.1–1 (b) and 0.005–0.5 nW (c). All else is as in Fig. 1.

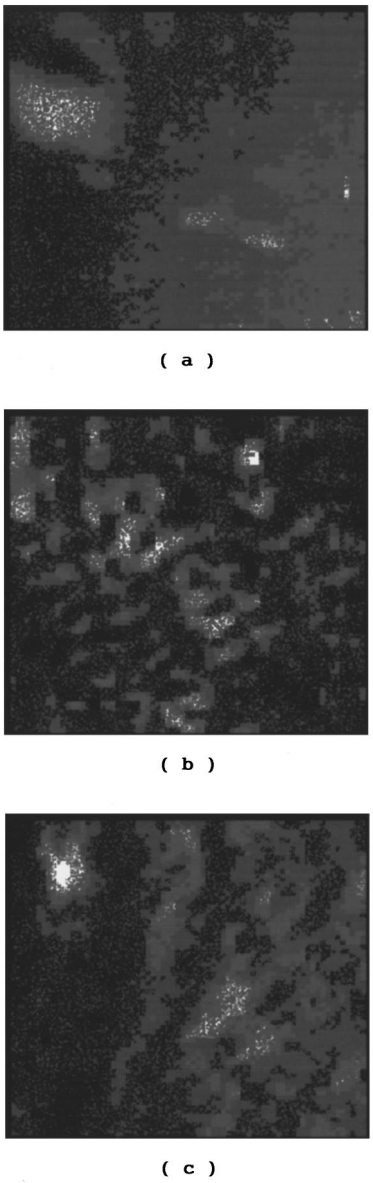

FIG. 3. Gray-scale topographical (a) and near-field optical (b) and (c) images 3×3 μm^2 obtained with film $G2$. The depth of the topographical image is 103 nm. The scales of optical images are $\sim$0.002–0.1 (b) and 0.02–0.06 nW (c). All else is as in Fig. 1.

scatter the SPP by reflecting it [cf. Fig. 1(b)] but rather transmitted the incident SPP, focusing it in an immediate vicinity of the scatterer. Even the SPP at λ_2 was observed to be focused in the same manner (Fig. 2) in spite of the extremely small propagation length. One can suggest that the focusing effect is similar to that of geodesic (or Luneburg) lenses known in integrated optics.[26] On the other hand, the bump is only a couple of wavelengths in size [Fig. 2(a)], and it might be more appropriate to consider the observed effect as a consequence of Mie scattering in two dimensions rather than as a conventional lens effect. One can notice that, even though $\lambda_1>\lambda_2$, the spot size of the focused SPP is smaller for λ_1 ($\sim$200 and 300 nm, respectively), whereas the intensity enhancement in the spot is larger for λ_2 ($\sim$5 and 10 times). Bearing in mind the Mie theory, one may conjecture that such a two-dimensional microlens for SPP's should exhibit a strong dispersion. Note that the spot size for λ_1 is noticeably less than $\lambda_1/2$ [Fig. 2(b)], a circumstance which indicates that two-dimensional near-field effects are involved in the formation of the focal spot.

The topography of film $G2$ and the SPP scattering at λ_1 have previously been studied in detail.[18,19] Film $G2$ has a typical island structure consisting of bumps with various heights (5–100 nm) and sizes (50–1000 nm) in the surface plane, and the surface scatterers are practically adjacent to each other. One can presume that $R\sim a\sim\lambda_1$ and, therefore, $L_1\gg l_1\sim\lambda_1$ (see Sec. II). In such a case, a strong localization of SPP's should be expected, and indeed this has been observed in the form of bright spots on the near-field optical images,[18,19] which are similar to those obtained during this study [Fig. 3(b)]. The enhancement ratio, size, and round shape of these bright spots, together with the fact that the spot positions did not correlate with the surface topography

and depended on the excitation angle, have been regarded as conclusive evidence of the strong localization of SPP's.[19] Thus, a difference in the topography between films $G1$ and $G2$ resulted in different scattering regimes at λ_1: single scattering and strong localization, respectively. Contrary to this case, the near-field optical images recorded at λ_2 with film $G2$ were of the same nature as those obtained with film $G1$, i.e., they showed a similar correlation with the local topography (cf. Figs. 3 and 1). This should have been expected, since $L_2 \sim \lambda_2$ and, therefore, the SPP's scattered by neighbor surface bumps, can hardly interfere with each other. The bright spot in the upper left corner of the optical image recorded at λ_2 [Fig. 3(c)] is most likely due to the aforementioned focusing effect (cf. Figs. 2 and 3). Note that this effect does not show up for λ_1 [Fig. 3(b)], probably because of multiple scattering and interference effects of the SPP's at λ_1. Dispersion of the focusing effect might also be at least partially responsible for the absence of this effect for λ_1.

B. Silver films

Typographical images of both silver films showed a smooth surface with μm-sized bumps separated on averaged by $R_1 \sim 7$ μm (film $S1$) and $R_2 \sim 5$ μm (film $S2$). For both films, excitation of the SPP's at both wavelengths exhibited a well-pronounced resonance behavior, and the average optical signal was more than 20 times smaller if the angle of incidence was out of resonance by $\sim 2°$. The signal under resonant excitation was about the same for both wavelengths, but slightly different for film $S1$ (~ 2 nW) and for film $S2$ (~ 0.5 nW). The observed differences in R and the average optical signal stem apparently from the difference in the fabrication procedures for these films. The SPP propagation length can be estimated as $L_1 \approx 22$ μm and $L_2 \approx 5.5$ μm for λ_1 and λ_2, respectively. In order to determine the regime of SPP scattering, these values should be compared with the values of the elastic-scattering mean free path l for the films. Assuming $a \sim 1$ μm [cf. Figs. 2(a) and 5(a) from Ref. 20] results in $l_1 \sim 50$ μm and $l_2 \sim 25$ μm (see Sec. II). Therefore, it was expected to observe the regime of single scattering for λ_2 with both films, and for λ_1 with film $S1$, whereas the SPP scattering at λ_1 with film $S2$ was presumed to appear as double scattering, resulting eventually in weak SPP localization. In fact, it turned out that, for the same film, the near-field optical images can be very different depending on the topography of the local surface area, and that images recorded with different films can be similar to each other with respect to the scattering regime.

Near-field optical images demonstrating the regime of single scattering for both wavelengths were usually obtained with film $S1$ (Fig. 4). Even though the image recorded at λ_1 exhibits a multiple interference pattern, it can be seen that the dominating scattered SPP's are, in fact, two single-scattered waves. These waves are presumably scattered by scatterers, which are located accordingly to the left and right of the imaged area. The scattered waves interfere with each other and with the excited SPP traveling upwards, but the interference fields related to the excited SPP are stronger than the field of their mutual interference (scattered waves are weaker than the incident one). The interference of the two scattered SPP's with the excited SPP results in a typical

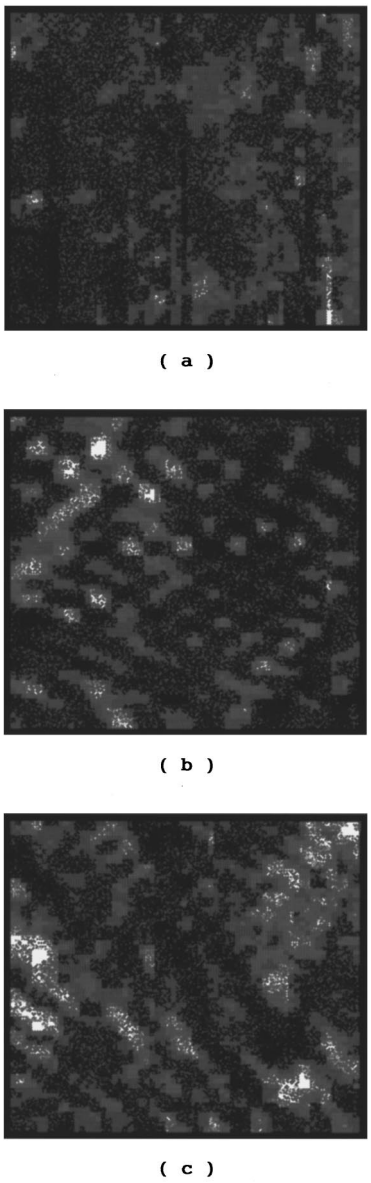

FIG. 4. Gray-scale topographical (a) and near-field optical (b) and (c) images 3×3 μm^2 obtained with film $S1$. The depth of the topographical image is 35 nm. The scales of optical images are ~ 0.1–1.2 (b) and 0.04–0.8 nW (c). All else is as in Fig. 1.

pattern similar to a crossed grating [Fig. 4(b)]. It appears that the scattered SPP's are of the same magnitude for λ_1 [Fig. 4(b)], whereas, for λ_2, the one propagating from the right is much stronger [Fig. 4(c)]. Using these two observations, one can conjecture that the left scatterer is located at a larger distance from the area imaged than the right scatterer and, in addition, that this distance is close to L_2. In general, the optical images recorded at λ_2 with film $S1$ were quite similar to those obtained at λ_1 with film $G1$ [cf. Figs. 1(b) and 4(c)], which could have been expected since the relevant values of L and l are nearly the same. Note that the observed interference patterns are superimposed with slow intensity variations correlated (somewhat differently for different wavelengths) with the surface topography (Fig. 4). This can be explained by the circumstance that the SPP excitation efficiency as well as the SPP radiative losses depend on the surface profile.

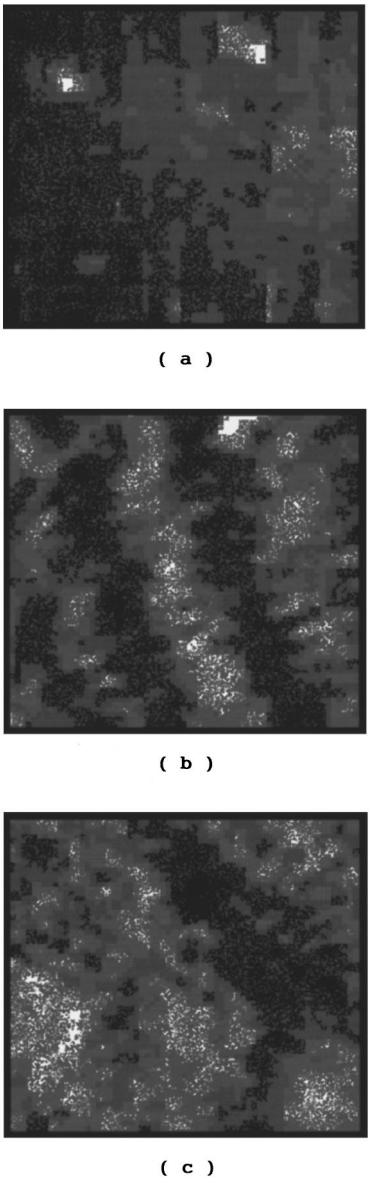

FIG. 5. Gray-scale topographical (a) and near-field optical (b) and (c) images $3\times3\ \mu m^2$ obtained with film $S2$. The depth of the topographical image is 23 nm. The scales of optical images are $\sim$0.1–0.4 (b) and 0.1–0.25 nW (c). All else is as in Fig. 1.

The near-field optical images demonstrating the regimes of single (for λ_2) and multiple (for λ_1) scattering were usually obtained with film $S2$ (Fig. 5). Well-pronounced intensity variations in the optical image at λ_2 have low spatial frequencies, and correlate with the appropriate topography variations [cf. Figs. 5(a) and 5(c)]. One can also notice a fine weak structure of the optical image at λ_2 that is similar to a crossed grating. This structure is mainly related to the interference of single-scattered SPP's and, in this respect, resembles that of the optical image recorded at λ_1 with film $S1$, even though the latter is much more pronounced than the former [cf. Figs. 4(b) and 5(c)]. This similarity is somewhat more surprising than the one mentioned above, since these two films have quite different values of the mean free path. However, the origin of the similarity is actually the same; that is, the ratio L/l, which determines the regime of scattering (see Sec. II), is not very different ($\sim$0.4 and 0.2 for λ_1 and for λ_2, respectively), and less than 1 in both cases. Note that the interference is less pronounced at λ_2 because of the shorter SPP propagation length. The structure of the optical image at λ_1 is much more complicated than that of the relevant image obtained with film $S1$ [cf. Figs. 4(b) and 5(b)]. This difference is attributed to the coherent multiple (mainly double) scattering of the SPP's. In such a case, it is expected that the phenomenon of weak localization should show up in the form of horizontal interference fringes related to the interference between excited and backscattered SPP's.[20] The considered optical image [Fig. 5(b)] does exhibit appropriate periodic intensity variations in the vertical direction, even though the horizontal fringes as such are not well pronounced.

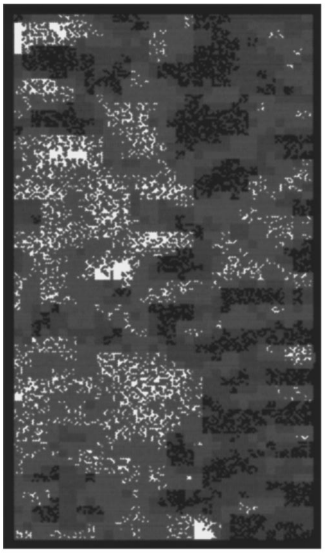

FIG. 6. The near-field optical image $1.5\times3\ \mu m^2$ obtained with film $S1$, and the polariton resonantly excited at $\lambda_1\approx633$ nm. The topography variation of the surface region imaged was less than 16 nm. The optical image is presented in the scale corresponding to $\sim$0.007–1.5 nW of the detected optical signal.

It has been pointed out[20] that a desirable interference pattern is difficult to observe due to the presence of other interference patterns related to different scattered SPP's. In three dimensions, measurements of backscattered light are carried out outside of a medium with randomly distributed scatterers.[4,5] Similarly, the formation of the backscattered SPP should be most pronounced relatively far away from individual scatterers, so that SPP's scattered along different routes would be of the same magnitude. From this point of view, both films have their own advantages (related to the fact that $l_1>l_2$): with film $S1$, it is easier to find the place relatively far away from surface scatterers, whereas, with film $S2$, it is easier to realize the regime of multiple scattering. Several examples of near-field optical images showing horizontal interference fringes have been previously obtained (at λ_1 with both silver films) and discussed in detail.[20] In the course of this study, a few optical images at λ_1 were also recorded with the purpose of finding the interference pattern related to the backscattered SPP. The best image showing the horizontal interference fringes was found with film $S1$ (Fig. 6). Still, it is seen that the horizontal fringes emerge from a rather complicated interference pattern and not just from in-

terference between the excited and backscattered SPP's. It should be noted that, except for some topographical images in which an average linear slope has been subtracted, the presented images are unprocessed.

V. CONCLUSIONS

Different regimes of elastic SPP scattering caused by surface roughness have been considered qualitatively. The possibility of realizing weak and strong localizations of SPP's in the surface plane has been related to the appropriate characteristics of SPP and surface roughness. Optical fields of SPP's excited along the surfaces of four different metal (silver and gold) films have been imaged simultaneously with surface topography by use of the photon scanning-tunneling microscope at two different wavelengths (488 and 633 nm) with shear force feedback. Single scattering and weak and strong localizations of SPP's have been observed depending on the sample and the light wavelength. The experimental results obtained have been found to be in agreement with our considerations. It has been shown that the regime of SPP scattering and, consequently, the near-field optical images, are determined by the topography of the local surface area within the SPP propagation length.

It has been found that strong localization of SPP's can be realized only at sufficiently strong disorder with $l \sim \lambda_{sp}$. This condition is close to the Ioffe-Regel condition for light localization in three dimensions, which is extremely difficult to fulfill.[27] On the other hand, the latter condition is stronger than the former one by 2π times. In addition, the divergence of the mean free path l in the Rayleigh limit (small scatterers, long wavelength) is weaker in two dimensions: $l \sim \lambda^3$ instead of λ^4 in three dimensions.[2] Resonance effects may also help to increase the scattering cross section and, consequently, to decrease the mean free path.[28] In fact, a strong localization of SPP's has been observed with a gold island film at a light wavelength of 633 nm,[18,19] and, in a similar arrangement, single-particle plasmons have been resonantly excited.[29] Apparently, a film surface should exhibit roughness in a sufficiently large range of sizes around the SPP wavelength,[19] a condition which can be formulated in a more quantitative way by using, for example, fractal surface characterization.[30]

Weak localization of SPP's can be realized with more or less standard vacuum-deposited films of an appropriately chosen metal (or the light wavelength), so that the SPP propagation length would be large enough: $L > l$. However, near-field observations of this effect have appeared cumbersome because of the superimposition of many interference patterns related to multiple-scattered SPP's. It should be borne in mind that single-scattered waves might have relatively strong components propagating in the direction of backscattering, which would produce interference fringes similar to those expected from the backscattered wave. An adequate theoretical consideration of the SPP scattering is desirable for an appropriate treatment of near-field optical images.

An interesting phenomenon in SPP scattering has been observed with different films and wavelengths; that is, focusing of the SPP by a surface bump of micron size into a subwavelength spot with the intensity enhancement by up to ~ 10 times. The focusing effect exhibited a strong dispersion, and seems to be related to Mie scattering in two dimensions. The microlens for SPP's as well as the previously observed microcavity[18] are certainly worth investigating further in order to develop a better understanding of these phenomena. Actually, one can envisage that micro-optics of SPP's might soon emerge as an exciting field with many interesting effects and various applications.

ACKNOWLEDGMENTS

The author is grateful to Dr. N. N. Novikova and Dr. A. V. Zayats (Institute of Spectroscopy, Troitsk, Russia) for providing the samples with silver films used in this study, and for helpful discussions.

[1] B. Souillard, in *Chance and Matter*, edited by J. Souletie, J. Vannimenus, and R. Stora (North-Holland, Amsterdam, 1987), p. 305.

[2] S. John, in *Scattering and Localization of Classical Waves in Random Media*, edited by P. Sheng (World Scientific, Singapore, 1990), p. 1.

[3] S. John, H. Sompolinsky, and M. J. Stephen, Phys. Rev. B **27**, 5592 (1983); S. John, Phys. Rev. Lett. **53**, 2169 (1984).

[4] M. P. van Albada, M. B. van der Mark, and A. Lagendijk, in *Scattering and Localization of Classical Waves in Random Media* (Ref. 2), p. 97.

[5] Yu. N. Barabanenkov *et al.*, in *Progress in Optics*, edited by E. Wolf (Elsevier, New York, 1991), Vol. 29, p. 65.

[6] E. Abrahams *et al.*, Phys. Rev. Lett. **42**, 673 (1979).

[7] K. Arya, Z. B. Su, and J. L. Birman, Phys. Rev. Lett. **54**, 1559 (1985).

[8] H. Raether, *Surface Plasmons*, Springer Tracts in Modern Physics Vol. 111 (Springer, Berlin, 1988).

[9] A. R. McGurn, A. A. Maradudin, and V. Celli, Phys. Rev. B **31**, 4866 (1985); A. R. McGurn and A. A. Maradudin, J. Opt. Soc. Am. B **4**, 910 (1987); J. A. Sanchez-Gil and M. Nieto-Vesperinas, Phys. Rev. B **45**, 8623 (1992); C. S. West and K. A. O'Donnel, J. Opt. Soc. Am. A **12**, 390 (1995), and references therein.

[10] O. A. Aktsipetrov *et al.*, Phys. Lett. A **170**, 231 (1992).

[11] A. R. McGurn, T. A. Leskova, and V. M. Agranovich, Phys. Rev. B **44**, 11 441 (1991).

[12] R. C. Reddick, R. J. Warmack, and T. L. Ferrel, Phys. Rev. B **39**, 767 (1989); D. Courjon, K. Sarayeddine, and M. Spajer, Opt. Commun. **71**, 23 (1989); F. de Fornel *et al.*, Proc. SPIE **1139**, 77 (1989).

[13] D. Van Labeke and D. Barchiesi, J. Opt. Soc. Am. A **10**, 2193 (1993).

[14] R. Carminati and J.-J. Greffet, Opt. Commun. **116**, 316 (1995).

[15] E. Betzig, P. L. Finn, and J. S. Weiner, Appl. Phys. Lett. **60**, 2484 (1992); R. Toledo-Crow *et al.*, *ibid.* **60**, 2957 (1992); A. Shchemelin *et al.*, Rev. Sci. Instrum. **64**, 3538 (1993).

[16] S. I. Bozhevolnyi, I. I. Smolyaninov, and O. Keller, Appl. Opt. **34**, 3793 (1995).

[17] O. Marti *et al.*, Opt. Commun. **96**, 225 (1993); H. Bielefeldt *et al.*, in *Near Field Optics*, edited by D. W. Pohl and D. Courjon (Kluwer, Dordrecht, 1993), p. 281; P. M. Adam *et al.*, Phys. Rev. B **48**, 2680 (1993); P. Dawson, F. de Fornel, and J. P. Goudonnet, Phys. Rev. Lett. **72**, 2927 (1994); D. P. Tsai *et al.*, *ibid.* **72**, 4149 (1994).
[18] S. I. Bozhevolnyi, I. I. Smolyaninov, and A. V. Zayats, Phys. Rev. B **51**, 17 916 (1995).
[19] S. I. Bozhevolnyi *et al.*, Opt. Commun. **117**, 417 (1995).
[20] S. I. Bozhevolnyi, A. V. Zayats, and B. Vohnsen, in *Optics at the Nanometer Scale*, edited by M. Nieto-Vesperinas and N. Garcia (Kluwer, Dordrecht, 1996), p. 163.
[21] E. Kretschmann, Z. Phys. **241**, 313 (1971).
[22] N. Kroo *et al.*, Surf. Sci. **331-333**, 1305 (1995).
[23] S. Etemad *et al.*, Phys. Rev. Lett. **59**, 1420 (1987).
[24] S. I. Bozhevolnyi, O. Keller, and M. Xiao, Appl. Opt. **32**, 4864 (1993).
[25] E. D. Palik, *Handbook of Optical Constants of Solids* (Academic, New York, 1985).
[26] D. L. Lee, *Electromagnetic Principles of Integrated Optics* (Wiley, New York, 1986).
[27] A. Z. Genack, Phys. Rev. Lett. **58**, 2043 (1987).
[28] K. Arya, Z. B. Su, and J. L. Birman, Phys. Rev. Lett. **57**, 2725 (1986).
[29] U. Ch. Fischer and D. W. Pohl, Phys. Rev. Lett. **62**, 458 (1989).
[30] S. I. Bozhevolnyi *et al.*, Surf. Sci. **356**, 268 (1996).